Induced and Inherent Anisotropies of Saturated and Unsaturated Soil Shear Properties

H. Toyota[1], B. N. Le[2] and S. Takada[3]
[1, 2, 3]Department of Civil and Environmental Engineering, Nagaoka University of Technology, Niigata, Japan
E-mail: toyota@vos.nagaokaut.ac.jp

ABSTRACT: Anisotropies of shear properties were examined for saturated and unsaturated soils. Induced anisotropy arises when an anisotropic stress is applied to a soil. Using a hollow cylinder torsional shear apparatus, cohesive saturated and unsaturated specimens were anisotropically consolidated in different directions. Then the shear strengths under an undrained condition for saturated soil and a constant water content condition for unsaturated soil were measured using those specimens. Inherent anisotropy develops from the orientation of soil particles during sedimentation. Specimens with different depositional angles were extracted from sand samples deposited in an inclined container. Finally, the shear properties under a drained condition for saturated sand and a constant suction condition for unsaturated sand were evaluated using the triaxial apparatus. The experimental results indicate that anisotropy, especially of the shear strength, is present for both the cohesive soil and the sand. However, shear strength anisotropy is lesser for the cohesive soil in the unsaturated condition than in the saturated condition.

KEYWORDS: Anisotropy, Cohesive soil, Matric suction, Sand, Torsional shear, Triaxial test, Unsaturated soil

1. INTRODUCTION

Casagrande and Corrilo (1944) defined two types of anisotropy in soils: (stress-) induced and inherent anisotropy. Induced anisotropy, which occurs when stresses and/or strains are applied to soils, is especially predominant in cohesive soils. Inherent anisotropy, which is engendered from soil particles' fabric created during soil sedimentation, is especially predominant in sandy soils.

It is well known that the shear strength is dependent on the direction of shear because of mechanical anisotropy of soils. The shear direction is changing even along one slip surface. For cohesive soils, Bjerrum (1972, 1973) demonstrated that strength properties are altered by stress conditions induced by triaxial compression, triaxial extension, and direct shear tests. Therefore, he recommended that suitable experiments which approximate the stress condition in the actual soil, should be used for ground stability analyses. Ladd and Foott (1974) conducted various shear tests using clay. The SHANSEP procedure, where the use of shear tests corresponding to the direction of shear is recommended, was developed to avoid unsafe conditions for design.

Studies have been made on specimens trimmed at various angles from a vertically consolidated remoulded clay sample (Mikasa et al., 1984) and from an undisturbed clay sample (Adachi et al., 1991). Mikasa et al. (1984) emphasized that unconfined compression strength decreased when a specimen's axial direction approaches the samples' horizontal directions. Results of undrained triaxial compression tests from Adachi et al. (1991) exhibited similar trends to those reported by Mikasa et al. (1984).

For sandy soils, Oda (1972) demonstrated that the inherent anisotropy is related to both the shape of the constituent grains and the mode of deposition. Arthur and Menzies (1972) investigated the inherent anisotropy caused by depositional angle differences. Yamada and Ishihara (1979) also conducted true triaxial tests on cuboidal loose sand specimens and found that inherent anisotropy strongly affected deformation characteristics of sand in the small shear strain range. Guo (2008), using results of modified direct shear tests with different angles of sedimentation, demonstrated that the particle shape and the direction of orientation dominated the degree of anisotropy. Tong et al. (2014) specifically examined inherent fabric anisotropy by investigating effects of the bedding plane on the peak friction angle using direct shear tests. Other studies (Oda et al., 1978; Ochiai and Lade, 1983; Wong and Arthur, 1985) have also revealed that inherent anisotropy has important effects on strength and stress–strain relationships of sands.

Detailed understanding of the anisotropy of saturated soils has been achieved and has been used to solve many geotechnical engineering problems such as underground structure design and ground deformation prediction. However, little knowledge exists on the anisotropy of unsaturated soils. Hence, the anisotropy of shear properties of saturated and unsaturated soils are examined in this study.

Torsional shear and triaxial tests were conducted using reconstituted cohesive soil and sand specimens to elucidate how strength anisotropy appears under saturated and unsaturated conditions. The specimens were anisotropically consolidated at various directions to create anisotropy for cohesive soil. For sand, the specimens' depositional angles were controlled in various directions. Moreover, mechanical properties of saturated and saturated soils were compared.

2. EXPERIMENTS

2.1 Materials

The cohesive soil used for this study is a lateritic soil designated as Yoneyama sandy silt. Yoneyama sandy silt includes grains of widely various sizes and contains no less than 20% sand. Toyoura sand, which is Japanese standard sand, was used as the test material for sand. Toyoura sand is a sub-angular to angular poorly graded fine quartz rich sand. Two principal dimensions (major axis L and minor axis W) of sand particles were measured from the 2-D optical microscope image to ascertain the sand particle shape. The sand particles are irregular circles because the aspect ratio L/W is distributed from 1.0 to 1.6; the average value of L/W is about 1.5 (Le et al., 2018). The grain size distribution curves and the physical properties of the soils are presented in Figure 1.

2.2 Specimen preparation

Yoneyama sandy silt and de-aired water were mixed and stirred well to produce slurry. The slurry water content was about 80%, which is about 1.6 times its liquid limit. Pre-consolidation using this slurry was performed one-dimensionally in a mould under 45 kPa vertical pressure. This vertical stress was selected from the minimum vertical stress at which the specimen can maintain its shape during trimming. The water content of the consolidated soil block was about 40%. The hollow cylindrical specimen, with 80 mm outer diameter, 50 mm inner diameter, and 160 mm in height, was formed by trimming from this soil block. The parameters, λ and κ, which respectively denote the slopes of normal compression and unloading–reloading lines in specific volume v and ln p' plane, were 0.072 and 0.014 under isotropic stress conditions for Yoneyama sandy silt.

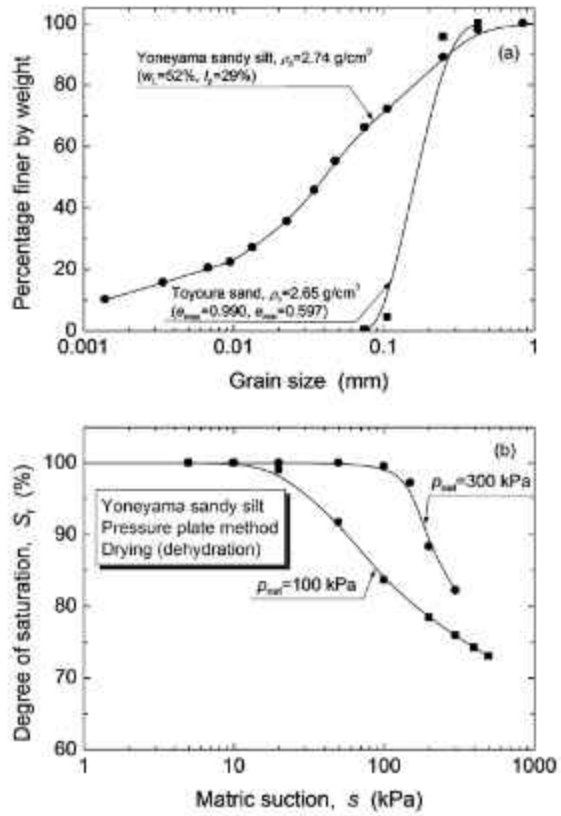

Figure 1 Testing soils: (a) grain size distributions and their physical properties and (b) water retention curves

Figure 2 depicts a rectangular container used to make samples of Toyoura sand with different depositional angles by changing the inclination and the position of its walls. Angles α of 0°, 22.5°, 45°, 67.5°, and 90° (Figure 2) were chosen as the depositional angles used for this study. The inherent anisotropy is related to the depositional process during soil particle sedimentation. Therefore, specimen preparation method plays a crucial role for mechanical properties of soil with inherent anisotropy. "Air pluviation" method was used to produce specimens with different depositional angles. Toyoura sand was poured into the container through a sieve with mesh size of 450 μm. The falling height of sand was kept constant at about 425 mm using a counter weight. Afterwards, the container full of sand was immersed in water for 2 hours. Then, water was removed. The remaining water in the sand sample was drained using a vacuum pump at -10 kPa. The sand sample produced using this method can stand by itself. Eventually, the cylindrical specimen, with 50 mm diameter and 125 mm height, was trimmed as shown in Figure 2 from the soil block under a basal plate being horizontally placed. This method can easily create a specimen with inclined depositional angle. The density of the specimen created was almost constant with relative density D_r of about 85%.

2.3 Test procedures

Test procedures are described in this section. As a preliminary test, the repeatability of the test performed was confirmed for some representative cases. The details of the apparatuses used are presented in the appendix.

2.3.1 Cohesive soil

The hollow-cylindrical torsional shear apparatus has a beneficial feature: it has shear directions that are changeable by control of stresses. The triaxial cell of the apparatus and its automatic control system are the same as those introduced by Toyota et al. (2001). A double-walled triaxial cell using an inner cell is introduced to measure the change of outer diameter when experiments are conducted on unsaturated soils. In this study, the inner cell was used to maintain full saturation of the specimen for a long time by placing a thin layer of silicone oil above the inner cell water to prevent air dissolution into the inner cell water. Toyota and Takada (2012) demonstrated that air dissolution of this type reduces the degree of saturation of the specimen.

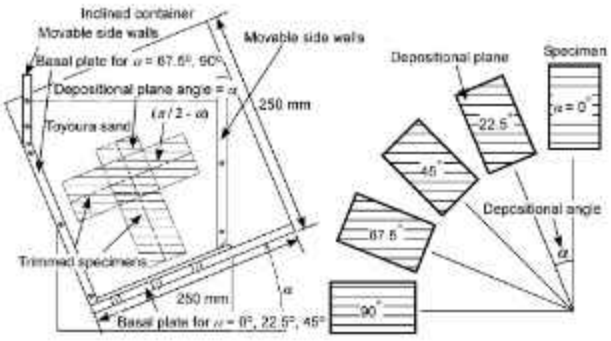

Figure 2 Inclined container and depositional angle

Angle α is the direction of the major principal stress relative to the vertical axis and b represents the relative magnitude of the intermediate principal stress. For instance, b=0 and b=1 respectively indicate stress conditions of triaxial compression and extension. The values of α and b were changed at K-consolidation and at shearing, which are differentiated, respectively, by subscript letters c and s. The stress conditions during shearing was fixed as α_s=45° and b_s=0.5 to minimise the effects of boundary conditions during shearing (Hight et al., 1983). Then, different α_c was set under b_c=0 condition during K-consolidation process. The unit "degree" is used as the unit of angle in this study.

Testing procedures are described below.

1. Isotropic consolidation process: The specimen was consolidated isotropically under p'=50 kPa with back pressure of 200 kPa (the B value was greater than 0.97) in the triaxial cell.
2. Drained q-loading process: After completing the isotropic consolidation, the specimen was sheared under drained conditions with strain control. Shear stress was applied up to $K(=\sigma_3/\sigma_1)$=0.35 under the stress condition of p'=50 kPa, a certain α_c and b_c=0. The rate of shear strain was about 0.0056%/min, where shear strain is defined as $\varepsilon_s = \sqrt{2}/3\sqrt{(\varepsilon_1-\varepsilon_2)^2+(\varepsilon_2-\varepsilon_3)^2+(\varepsilon_3-\varepsilon_1)^2}$.
3. Drying process: This process was skipped for the saturated specimen. Matric suction, $s = (u_a - u_w)$, of 400 kPa was applied to the specimen for drying under constant q and $p_{net} = (p - u_a)$ in the axis-translation technique using a ceramic disk. About 5 days is for the drainage from the ceramic disk to become less than 0.2 cm^3/day.
4. K-consolidation process: The specimen was consolidated under a constant K with the same α_c and b_c as the drained q-loading process, up to p' or p_{net} of 300 kPa. The loading rate during this process was controlled with an almost identical rate of shear strain as that of the drained q-loading process.
5. Drained q-unloading process: Shear stress was unloaded up to isotropic stress conditions of 300 kPa under drained conditions.
6. Shearing process: Torsional shearing was conducted under undrained condition and under constant water content (CW) condition in saturated and unsaturated soils, respectively, with stress conditions of a constant p' or p_{net}, α_s=45°, and b_s=0.5. The rate of shear strain were 0.01%/min in saturated and unsaturated soils.

The shear direction is an important factor that must be considered for the anisotropic shear strength on actual ground. Its importance exists in the difference in directions, which is denoted as $\alpha' = |\alpha_c - \alpha_s|$, between the K-consolidation and the shearing.

2.3.2 Sand

A series of experiments using the triaxial apparatus was conducted to estimate the effects of the inherent anisotropy on shear strength and deformation characteristics. A bender element (BE) was installed in the apparatus to estimate the initial shear modulus G_0 from the shear wave velocity. The BEs are mounted on the top cap (transmitter function) and on the pedestal (receiver function). The BE dimensions are 2.5 mm length, 12 mm width, and 1 mm thickness. The BE tests were uniformly carried out based on a standard of Japanese Geotechnical Society (2011).

Local small strain (LSS) technique was incorporated into the apparatus to measure the small strain and also radial strain for unsaturated soils accurately (Le et al., 2018). Two separate targets were glued directly on the membrane to measure the vertical axial displacement. A couple of proximity transducers were fastened on two columns near the specimen. Distances between the targets and the proximity transducers can be adjusted from outside of the triaxial cell. The distance between the two targets was about 80 mm. To measure the radial strain, the proximity transducer was installed in the middle part of the specimen using a clamping device.

Testing procedures are described below.

1. The prepared specimen was placed into the triaxial cell. Initially, suction of -20 kPa was applied to the specimen. The double vacuum method was used for saturation.
2. Maintaining suction of -20 kPa inside the specimen, cell water was removed from the triaxial cell. Specimen dimensions were then measured carefully. Transducers for LSS were installed in the triaxial cell to avoid affecting the specimen condition.
3. After supplying cell water in the triaxial cell, the suction was decreased while the cell pressure was increased so that the isotropic effective stress was maintained constant at 20 kPa. Then, backpressure of 200 kPa was applied to increase the degree of saturation of the specimen: the B value was greater than 0.98.
4. In the isotropic consolidation process, effective stress of 150 kPa was applied to the specimen. Then the BE test was conducted by input of a single sinusoidal wave with frequencies of 15 kHz, 20 kHz, and 30 kHz to ascertain the shear wave velocity.
5. Matric suction, $s = (u_a - u_w)$, of 50 kPa was applied to the specimen for drying under constant $p_{net} = (p - u_a)$ in the axis-translation technique using a ceramic disk. About 2.5 days were necessary for drainage from the ceramic disk to become less than 0.2 cm^3/day. The degree of saturation S_r of the specimen became about 17%. This process was skipped in the saturated specimen. Then the BE test was conducted.
6. Monotonic compression was conducted under a drained condition for saturated sand and constant suction (CS) condition for unsaturated soil at a constant cell pressure and constant axial strain rate of 0.05%/min for tests to ascertain the shear strength.

3. TEST RESULTS

3.1 Saturated cohesive soil

In the hollow-cylindrical torsional shear apparatus, the saturated specimens were consolidated at K=0.35 with various directions. Then the specimens were sheared under an undrained condition to elucidate the stress-induced anisotropy. The stress–strain relations and the stress paths are depicted, respectively, in Figures 3(a) and 3(b). The void ratios just before the shearing were almost the same in all cases, which was 0.837. When the value of α' becomes greater, the deviator stress, $q = 1/\sqrt{2}\sqrt{(\sigma_1 - \sigma_2)^2 + (\sigma_2 - \sigma_3)^2 + (\sigma_3 - \sigma_1)^2}$, reaches a smaller value. The reason can be inferred from the result of the stress paths. The generation of pore-water pressure is greater when α' is greater. Therefore, the failure state appears at smaller $p' = (\sigma_1 + \sigma_2 + \sigma_3) / 3$ in the case of greater α'. Actually, q grows gradually along the failure line after reaching the failure line because the specimen contains a sand fraction. However, in practice (in actual soil), maintaining a perfectly undrained condition under dilative behaviour is uncertain. Screening unsafe designs, Toyota et al. (2014) defined the shear strain to estimate the undrained shear strength as the shear strain at which the stress path reached the failure line in the case of α'=0. The same method was used in the present study. The circle markers in Figures 3(a) and 3(b) show shear strain defined using this method.

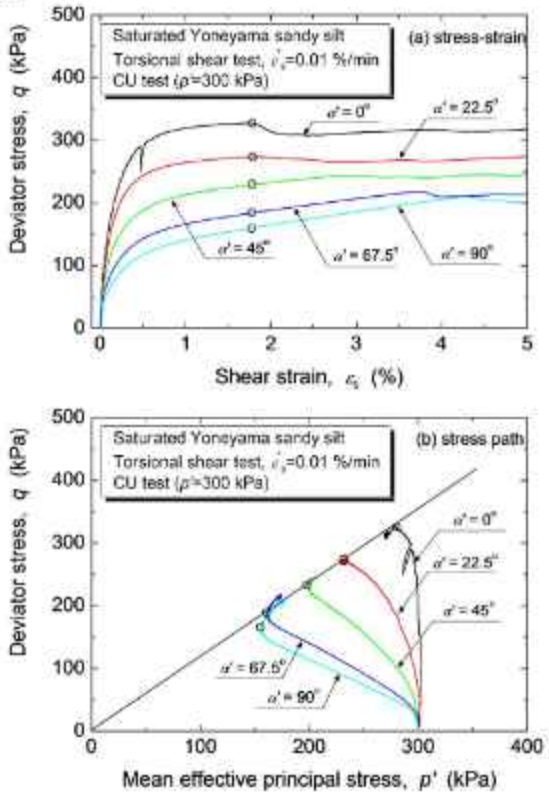

Figure 3 Undrained shear properties of saturated cohesive soil: (a) stress–strain and (b) stress path

Figure 4 presents the relation between the undrained shear strengths of the saturated cohesive soil and the directional difference between K-consolidation and shearing, α'. The undrained shear strengths are decreasing with increased α'. Toyota et al. (2014) reported the undrained strength decrease line of this kind under K_0 (=0.43) condition. The line is added to the figure. Greater difference through α' appears in the K=0.35 than K=0.43 conditions, meaning that a small K engenders strong anisotropy in undrained shear strength of the cohesive soil.

3.2 Unsaturated cohesive soil

Figures 5(a), 5(b), and 5(c), respectively, show the stress–strain, volumetric strain and matric suction behaviour with shear strain under CW condition. The void ratios just before the shearing were almost the same in all cases, which was 0.774. The difference is not readily apparent but the following tendency is apparent. When the value of α' becomes greater, the peak deviator stress becomes smaller. The peak deviator stress appears at smaller shear strain with a smaller value of α'. Strain softening is apparent in the stress–strain relations. The volumetric strain exhibits more contraction for greater α' and more dilation for smaller α' (Figure 5(b)).

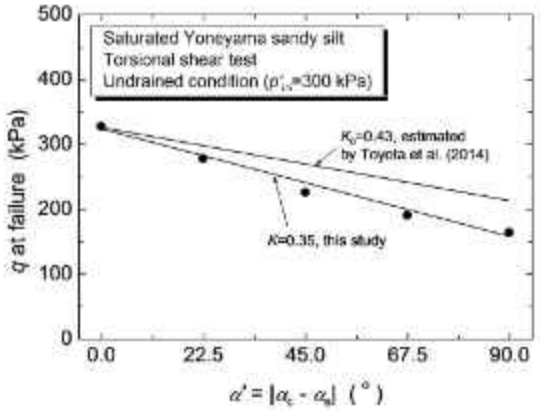

Figure 4 Undrained shear strength of saturated cohesive soil

The matric suction changes during shearing are presented in Figure 5(c). The matric suction tends to decrease greatly at greater α', which demonstrates anisotropic shear properties with respect to the matric suction. The values of the matric suction decrease sharply within shear strain of 1%. After shear strain of 1%, the matric suction values scarcely vary and maintain at about 200 kPa. Although change in the degree of saturation was slight because of the CW condition, the change of matric suction during shearing was large, such as a change from 400 kPa to 200 kPa. Some doubt persists as to whether the matric suction change was induced by shearing alone. Therefore, the matric suction was monitored continuously under an undrained condition before shearing. The monitoring results show that the matric suction decreases gradually, but it tends to converge with time (Figure 6) because drainage of 0.2 cm^3/day remains after the drying process. However, this change of matric suction (Figure 6) is less than that during shearing, implying that a large part of the matric suction change occurred during shearing.

Figure 7 presents the relation between the shear strengths of the unsaturated cohesive soil under CW condition and α'. Except for application of the matric suction, the same anisotropic stresses as those of saturated specimens act on the specimens. The shear strength change is divided into two parts: the decreasing shear strength part for α' from 0° to 45° and the constant shear strength part for α' from 45° to 90°. Figure 4 shows that the change of the shear strength, which implies induced anisotropy, is much less than that in the saturated cohesive soil under an undrained condition.

3.3 Saturated sand

The preparation method used for the study might create a different depositional angle with similar relative densities of about 85%. Dense sand exhibits clear peak strength and strain softening because of the dilatancy induced by interlocking of the sand particles.

Figures 8(a) and 8(b), respectively, present the stress–strain and the volumetric strain versus shear strain relations in saturated sand under drained conditions. Shearing was halted at the shear strain of about 10% because of the interference of LSS measuring devices. According to Figure 8(b), the specimen did not reach the steady state in this strain range. The peak strength appeared at smaller shear strain when α is smaller. There are apparent effects of the depositional plane angle on shear behaviour. The shear strength becomes smaller with increased α. However the volumetric behaviour is similar and independent of α. Sand particles will deposit with their major axis reclined horizontally during air pluviation. Therefore, greater shear strength appears when sand particles recline horizontally in triaxial compression tests.

Relations between the drained shear strength and the depositional angles are presented in Figure 9. The depositional angle α markedly affects the drained shear strength of sand. The drained shear strength becomes smaller when α changes from a horizontal to vertical depositional angle. However, the drained shear strengths of α=67.5° and 90° are almost equal because the lowest strength appears in the direction of the "potential" strain localization plane based on the Mohr–Coulomb failure criterion, as demonstrated in plane strain tests (Oda et al., 1978; Tatsuoka et al., 1986).

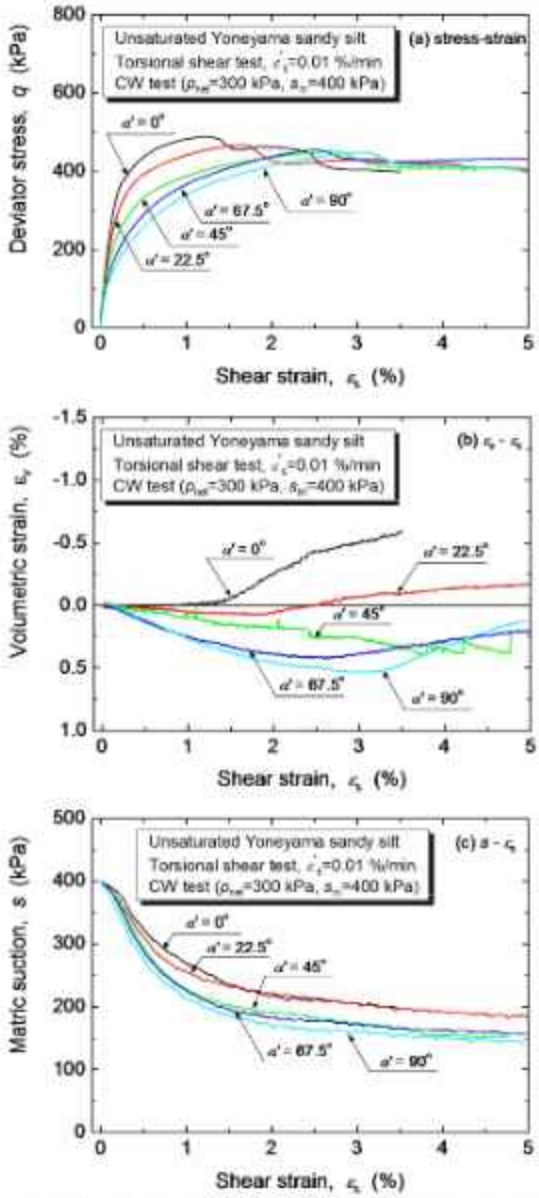

Figure 5 Shear properties of unsaturated cohesive soil under CW condition: (a) stress–strain, (b) volumetric strain, and (c) matric suction

The initial (maximum) shear modulus was estimated from the result of the bender element (BE) test. The relation between the initial shear modulus and α is presented in Figure 10. The data in Figure 10 are somewhat scattered, but G_0 increases slightly with increased α. It is interesting that although apparent anisotropy appears in the drained shear strength (Figure 9), slight anisotropy, which has reverse relation relating to the effect of α with the drained shear strength, arise in the initial shear modulus estimated from BE test. Mechanisms of anisotropy are expected to be different between shear strength (adequate strain level) and the initial shear modulus (very small strain).

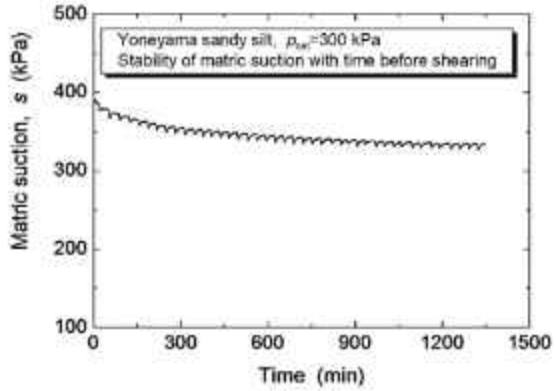

Figure 6 Stability of matric suction with time

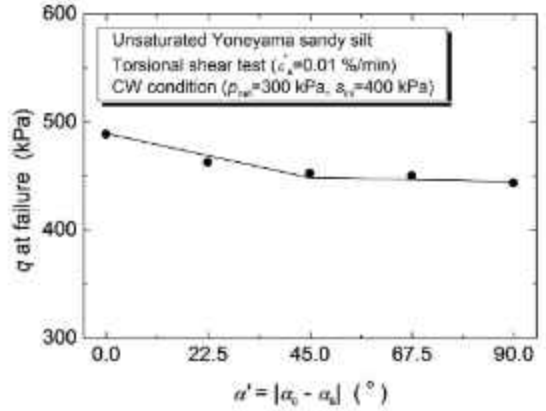

Figure 7 Shear strength of unsaturated cohesive soil under CW condition

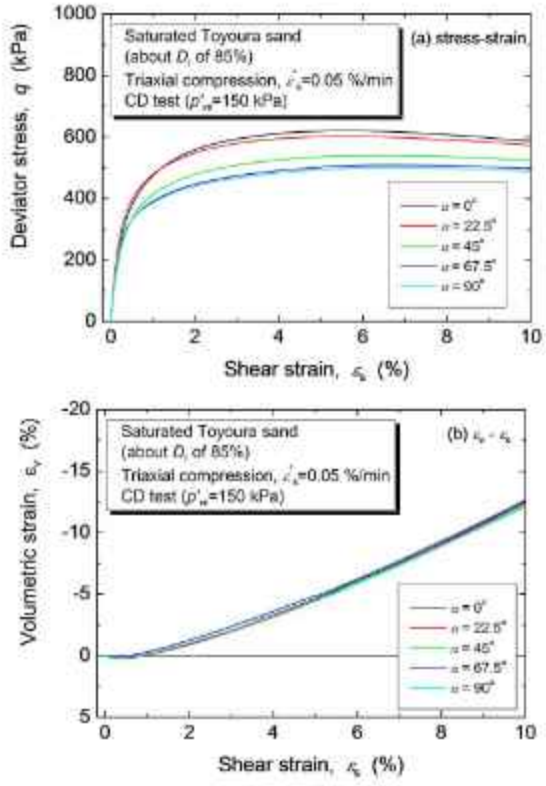

Figure 8 Drained shear properties of saturated sand: (a) stress–strain, and (b) volumetric strain

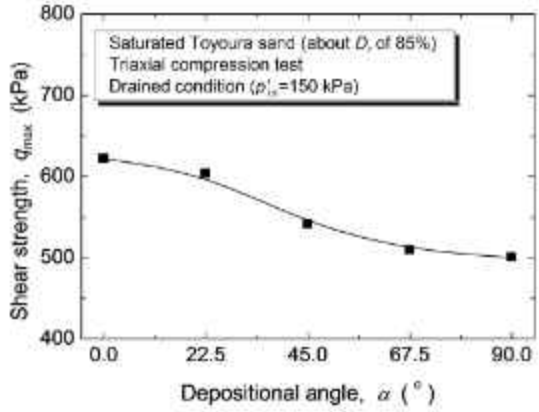

Figure 9 Drained shear strength of saturated sand

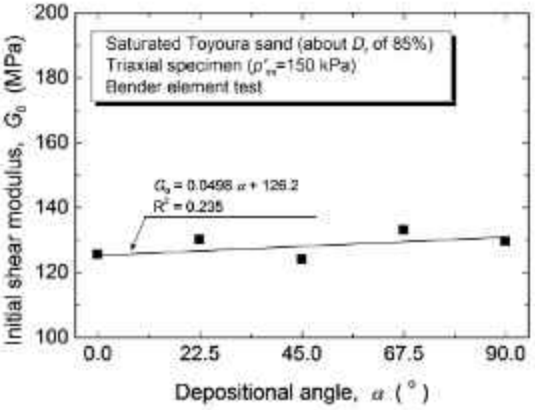

Figure 10 Initial shear modulus of saturated sand

3.4 Unsaturated sand

Figures 11(a) and 11(b), respectively, portray the stress–strain and the volumetric strain versus shear strain relations in unsaturated sand under constant suction (CS) conditions. The limitation of maximum shear strain is the same as the saturated sand. The same tendency as that the saturated sand appears in shear behaviour: 1. The peak strength appeared at smaller shear strain in the case of smaller α. 2. The shear strength becomes small with increased α. 3. The volumetric behaviour is similar and independent of α. However, the dilative tendency seems to lessen slightly with increased α in the unsaturated sand. Therefore, the anisotropic shear behaviour was observed not only in saturated sand but also unsaturated sand.

Figure 12 presents relations between the shear strength of unsaturated sand under a CS condition and the depositional angles. The depositional angle effect on the shear strength of unsaturated sand is the same as the drained shear strength in saturated sand: the shear strength becomes smaller when α changes from a horizontal to a vertical depositional angle. The applied matric suction of 50 kPa to the sand specimen does not affect the tendency of anisotropic behaviour in drained shear strength.

Figure 13 shows the relation between the initial shear modulus obtained from the BE test and α. This relation shows the same tendency as that for saturated sand: the initial shear modulus slightly increases with increased depositional angle α. Reverse anisotropy with that in the drained shear strength appears in the initial shear modulus, while its anisotropy is not obvious comparing with that in the shear strength of unsaturated sand (Figure 12).

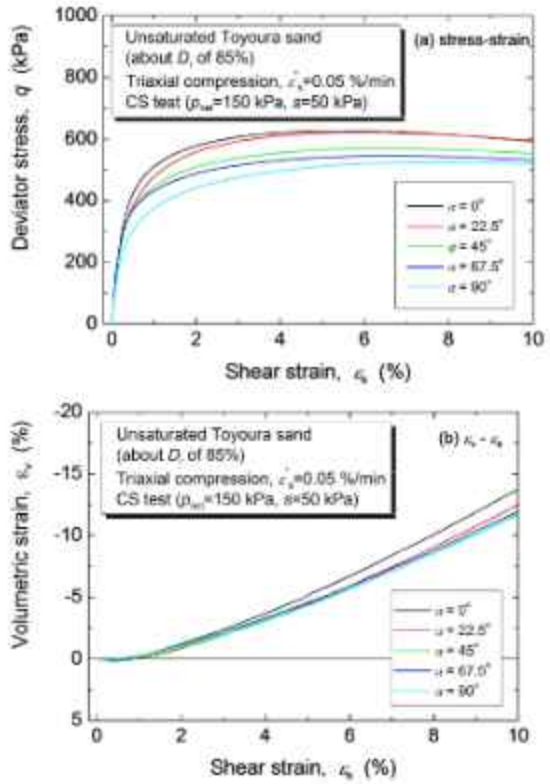

Figure 11 Shear properties of unsaturated sand under CS condition: (a) stress–strain and (b) volumetric strain

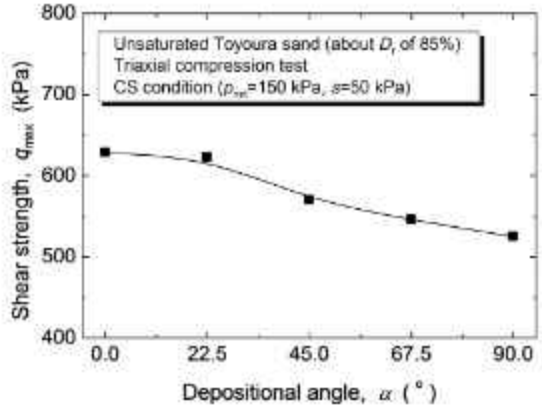

Figure 12 Shear strength of unsaturated sand under CS condition

3.5 Comparison between saturated and unsaturated soil

Figure 14 portrays the shear strengths and α' for cohesive soil under undrained and CW conditions. Differences between saturated and unsaturated soils are induced by application of the matric suction of 400 kPa. Significant differences appear from the matric suction in the cohesive soil. It is interesting that the undrained shear strength decays by about 50% with the increase of α', but it decays only by 10% in the unsaturated soil, indicating that the strength anisotropy is more remarkable in the saturated soil than in the unsaturated soil. Therefore, the strength anisotropy is less important for unsaturated cohesive soils in practice.

Fredlund et al. (1978) expressed the failure of unsaturated soils using two independent stress variables $(\sigma - u_a)$ and $(u_a - u_w)$ as follows:

$$\tau = c' + (\sigma - u_a)\tan\phi' + (u_a - u_w)\tan\phi^b \quad (1)$$

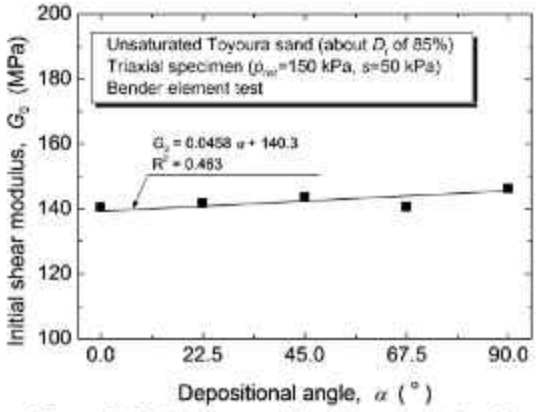

Figure 13 Initial shear modulus of unsaturated sand

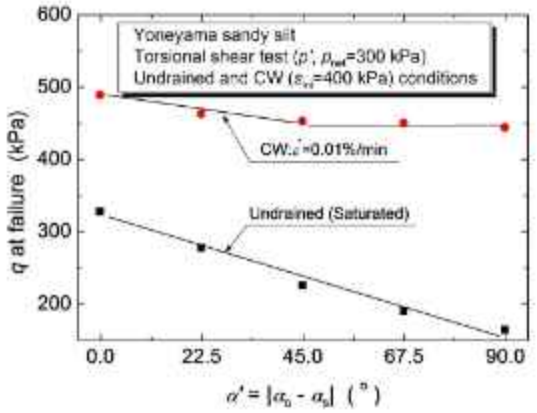

Figure 14 Shear strength of saturated and unsaturated cohesive soils

Data obtained from this study were applied to the failure equation. Here, the data of the saturated soil were regarded as replacing the excess pore water pressure as the negative matric suction. The values of the shear strength and the matric suction were extracted at failure points as defined previously. They are presented in Figure 15. Roughly linear relations but different inclinations are obtained in each part of the saturated and the unsaturated states. The intersectional point between the two lines represents an air entry value (AEV), which is the matric suction at which the air starts to enter the soil specimen. Finally, $c' = 0$, $\phi' = 43.6°$ and $\phi^b = 11.2°$ in equation (1) were calculated from the results. Therefore, the shear strength can be estimated from equation (1) when the change of the matric suction or pore water pressure is found at the failure point.

Next, the shear strength and the initial shear modulus of sand were inferred from comparison between saturated and unsaturated conditions. Figure 16 shows the respective relations between the shear strengths and α for sand under drained and CS conditions for the saturated sand and the unsaturated sand. The difference between the saturated sand and the unsaturated sand is induced by application of 50 kPa matric suction. The drained shear strength of unsaturated sand is slightly greater than that of saturated sand. This is a smaller difference than that for cohesive soil because of the small suction effect induced by large soil grains. The saturated sand and the unsaturated sand show similar tendencies, meaning that the matric suction affects the shear strength to the same degree irrespective of the inherent anisotropy induced by the sand particle orientation. Therefore, the strength of unsaturated sand can be estimated by adding the suction effect to the strength of the saturated sand.

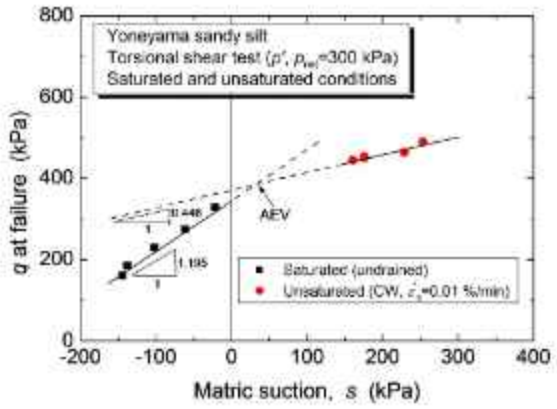

Figure 15 Shear strength induced by matric suction

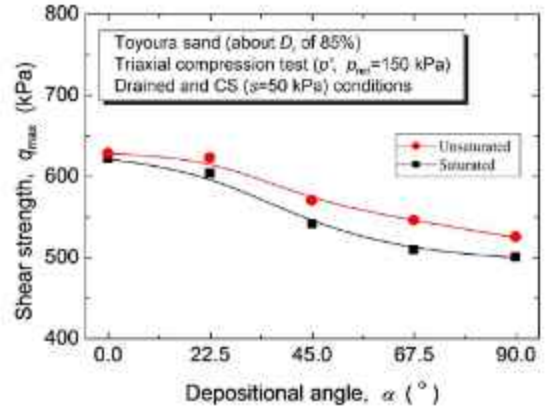

Figure 16 Shear strength of saturated and unsaturated sands

Figure 17 shows the respective relations between the initial shear modulus and α for sand under drained and CS conditions for the saturated sand and the unsaturated sand. The only difference between the saturated sand and the unsaturated sand is whether the matric suction of 50 kPa is applied to the specimens or not. Although the data scatter to some degree, the matric suction slightly increases the initial shear modulus without change of the trend between initial shear modulus and α. This is the same as that of the drained shear strength. Therefore, the effect of matric suction is the same for both the shear strength and the initial shear modulus.

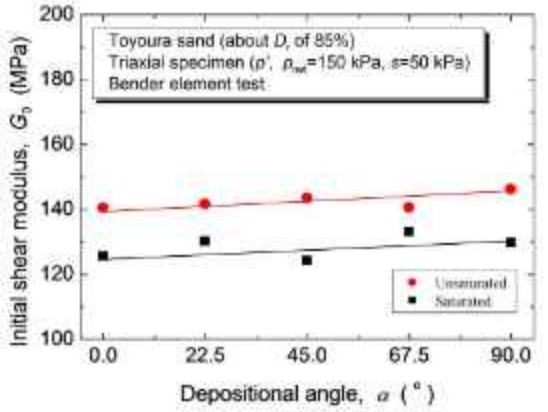

Figure 17 Initial shear modulus of saturated and unsaturated sands

4. CONCLUSIONS

The (stress-) induced and inherent anisotropy were investigated, respectively, using specimens of Yoneyama sandy silt and Toyoura sand. Induced anisotropy was generated from stress acting on the specimen. The inherent anisotropy was expressed in the specimen extracted from a sample where sand was reconstituted with different depositional angles in an inclined container. The anisotropy effects on mechanical properties of saturated soils and unsaturated soils were examined and discussed. Results led to the following conclusions.

1. The strength anisotropy developed in the specimens sheared under undrained conditions for the saturated cohesive soil and under CW conditions for the unsaturated cohesive soil. The shear strength dropped by about 50% with the greatest difference of α' in the saturated cohesive soil. For the unsaturated cohesive soil, that is about 10%. The inclination of the stress–strain curve decreased with increased α'.
2. Strength anisotropy was generated, respectively, from the change of pore water pressure and matric suction in the saturated cohesive soil and in the unsaturated cohesive soil. Therefore, when the change of the pore water pressure or the matric suction during shearing can be known at the failure point, the shear strength can be calculated using existing failure criteria.
3. The shear strength of sand under a drained condition for the saturated sand and under a CS condition for unsaturated sand markedly decreases with an increase of the depositional angle.
4. The initial shear moduli of both saturated and unsaturated sands are slightly increased with increased depositional angle α. This is an opposite tendency from that reported for the effect of α on the drained shear strength. The initial shear modulus of sand increases slightly by the application of matric suction.
5. The matric suction effect on the shear strength is smaller between the saturated sand and the unsaturated sand than that in the cohesive soil.

5. ACKNOWLEDGEMENTS

Experiments presented herein were conducted assisted by former graduate students at the Geotechnical Engineering Laboratory, Department of Civil and Environmental Engineering, Nagaoka University of Technology. The authors deeply appreciate their experimental assistance and helpful cooperation.

6. REFERENCES

Adachi, T., Oka, F., Hirata, T., Hashimoto, T., Pradhan, T. B. S., Nagaya, J., and Mimura, M. (1991). "Triaxial and torsional hollow cylinder tests of sensitive natural clay and an elasto-viscoplastic constitutive model". Proc. Tenth European Conference on SMFE, 1, pp. 3–6.

Arthur, J. R. F., and Menzies, B. K. (1972) "Inherent anisotropic in sand. Géotechnique". 22(1), 115-125.

Bjerrum, L. (1972) "Embankments on soft ground". Specialty Conference on Performance of Earth and Earth Supported Structures, ASCE, 2, pp. 1–54.

Bjerrum, L. (1973) "Problems of soil mechanics and construction on soft clays and structurally unstable soils". Proc. Eighth ICSMFE, 2, pp. 111–159.

Casagrande, A., and Carillo, N. (1944) "Shear failure of anisotropic material". J. Boston Soc. Civ. Eng., 31(4), 74–87.

Guo, P. (2008) "Modified direct shear test for anisotropy strength in of sand". Journal of Geotechnical and Geoenvironmental Engineering, 134(9), 1311–1318.

Hight, D. W., Gens, A. and Symes, M. J. (1983) "The development of a new hollow cylinder apparatus for investigating the effects of principal stress rotation in soils". Géotechnique, 33(4), 355–383.

JGS standards (2011) "JGS 0544-2011 Method for laboratory measurement of shear wave velocity of soils by bender element". Laboratory Testing Standards of Geomaterials, 3, Japanese Geotechnical Society (JGS).

Ladd, C. C., and Foott, R. (1974) "New design procedure for stability of soft clays". Journal of the Geotechnical Engineering Division, ASCE, 100(GT7), 763–786.

Le B. N., Toyota, H., and Takada, S. (2018) "Detection of elastic region varied by inherent anisotropy of reconstituted Toyoura sand". In: Wasowski J., Giordan D., Lollino P. (eds) Engineering Geology and Geological Engineering for Sustainable Use of the Earth's Resources, Urbanization and Infrastructure Protection from Geohazards. GeoMEast 2017. Sustainable Civil Infrastructures. Springer, Cham. https://doi.org/10.1007/978-3-319-61648-3_5

Mikasa, M., Takada, N., and Ohshima, A. (1984) "Anisotropy of undrainde strength of one-dimensionally consolidated clay and natural clay deposits". Tsuchi-to-Kiso, JGS, 32(11), 25–30 (in Japanese).

Ochiai, H., and Lade, P. V. (1983) "Three-dimensional behavior of sand with anisotropic fabric". Journal Geotechnical Engineering, 109(10), 1313–1328.

Oda, M. (1972) "Initial fabrics and the relations to mechanical properties of granular material". Soils and Foundations, 12(1), 17–37.

Oda, M., Koishikawa, I., and Higuchi, T. (1978) "Experimental study of anisotropic shear strength of sand by plane strain test". Soils and Foundations, 18(1), 25–38.

Tatsuoka, F., Sakamoto, M., Kawamura, T., and Fukushima, S. (1986) "Strength and deformation characteristics of sand in plane strain compression at extremely low pressure". Soils and Foundations, 26(1), 65–84.

Tong, Z., Zhou, S., Fu, F., and Dafalias, F. Y. (2014) "Experimental investigation of shear strength of sands with inherent fabric anisotropy". Acta Geotechnica, 9(2), 257–275.

Toyota, H., Sakai, N., and Nakamura, K. (2001) "Mechanical properties of saturated cohesive soil with shear history under three-dimensional stress conditions". Soils and Foundations, 41(6), 97–110.

Toyota, H., Susami, A., and Takada, S. (2014) "Anisotropy of undrained shear strength induced by K_0 consolidation and swelling in cohesive soils". International Journal of Geomechanics, ASCE, 14(4), 04014019-1 – 04014019-17.

Toyota, H., and Takada, S. (2012) "Technique for undrained triaxial tests on unsaturated soils using active control of pore-air pressure". Geotechnical Testing Journal, ASTM, 35(3), 480–489.

Wong, R. K. S., and Arthur, J. R. F. (1985) "Induced and inherent anisotropy in sand". Géotechnique, 35(4), 471–481.

Yamada, Y., and Ishihara, K. (1979) "Anisotropic deformation characteristic of sand under three-dimensional stress conditions". Soils and Foundations, 19(2), 79–94.

7. APPENDIX

Figures and photos of the test apparatuses are schematically shown in this section. The hollow cylinder torsional shear apparatus is depicted in Fig. A-1 and Photo A-1. Setting of the local strain measurements incorporated in triaxial apparatus is represented in Fig. A-2 and Photo A-2.

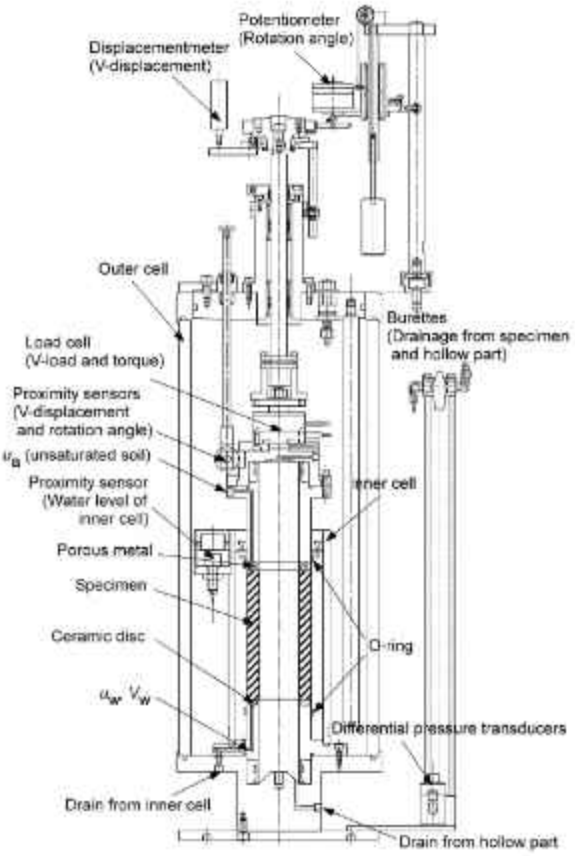

Figure A-1 Triaxial cell of hollow cylinder torsional shear apparatus

Photo A-1 Triaxial cell of hollow cylinder torsional shear apparatus

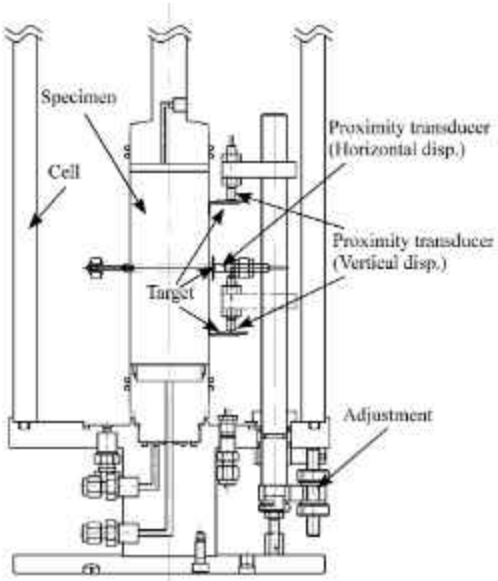

(a) Side view

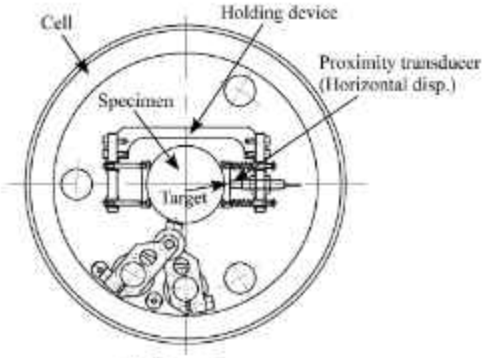

(b) Plan view

Figure A-2 Local strain measurements for triaxial apparatus

Photo A-2 Local strain measurements for triaxial apparatus